

## Aggregation, Fragmentation, and the Nonlinear Dynamics of Electrorheological Fluids in Oscillatory Shear

James E. Martin and Judy Odinek

*Advanced Materials Physics Division, Sandia National Laboratories, Albuquerque, New Mexico 87185-1421*  
(Received 17 November 1994)

We have conducted a time-resolved, two-dimensional light scattering study of the nonlinear dynamics of field-induced structures in an electrorheological fluid subjected to oscillatory shear. We have developed a theoretical description of the observed dynamics by considering the response of a fragmenting and aggregating particle chain to the prevailing hydrodynamic and electrostatic forces. This structural theory is then used to describe the nonlinear rheology of electrorheological fluids.

PACS numbers: 47.50.+d, 82.70.Dd, 83.50.Sp

Electrorheological (ER) fluids are particle suspensions that undergo dramatic rheological changes when subjected to strong electric fields [1,2]. The rheology of these fluids at low to moderate volume fractions is due to the aggregation of particles into volatile chainlike structures whose size adjusts in response to the flow, fragmenting and aggregating as the shear rate increases or decreases.

Structural studies on ER fluids have focused on the quiescent state and on stationary flows. Optical studies of the quiescent ER fluid have elucidated both the kinetics of structure formation [3] and the final equilibrium state [4]. Light scattering studies of an ER fluid in steady shear [5] have determined the manner in which the chain size and orientation increases with shear rate, confirming earlier experiments and theory of the power-law shear thinning viscosity [6].

Although some experimental work has been done on fluid structure in stationary flows, the chain dynamics has not yet been determined in nonstationary flows such as oscillatory shear. Because an understanding of electrorheology in nonstationary flows is essential to modeling the behavior of ER devices, we have undertaken a study of the chain dynamics in oscillatory shear. We have discovered a class of nonlinear dynamics that is dominated by fragmentation and aggregation events occurring during each shear cycle, and have used our observations to develop a theory of nonlinear rheology. Direct rheological measurements [7,8] show that the framework of linear viscoelasticity—a phase-shifted stress proportional to an applied strain—is of limited utility for ER fluids, and so a nonlinear theory is appropriate.

*Sample preparation.*—Our sample is a transparent model silica fluid developed for light scattering and rheology studies [3]. The 700 nm spheres are coated with a silane coupling agent and dispersed in 4-methylcyclohexanol to 7.5 wt % silica. Aggregation is reversible by Brownian motion.

*Apparatus.*—The scattering cell consists of an inner  $40 \times 2$  mm circular disk electrode that is concentric to a 42 mm hole in an outer electrode, thus creating a radial electric field in a 1 mm gap. The outer electrode is sand-

wiched between plastic, and both are embedded between glass plates, with a fluid-filled 2 mm gap between the electrodes and the glass plates. The inner electrode is oscillated by a rod connected to a 25 mm lever on the electrode shaft, driven by an eccentric on a 300 oz in. microstepping motor.

The electric field is a 1 kHz square wave from a Trek power supply driven by a Wavetek signal generator. Voltages are reported peak to peak. Scattering data are captured by a Pulnix video camera, and stored on video tape. Data are then digitized in real time by a Perceptix frame grabber on a Macintosh Quadra 950. Optical corrections are then made to the scattering data [3].

A problem in this experiment is the phasing of the applied strain with the scattering data. We devote a small corner of the scattering screen to an optical “strain phase clock” created by a prism rotating in synchrony with the stepping motor. The prism deflects a He-Ne laser beam that thus scribes a circle on the scattering screen, encoding the absolute strain phase on each image.

*Data analysis.*—A scattering image contains a pair of scattering lobes [3] and the strain phase clock. These scattering lobes are tilted relative to the orientation of the scattering lobes obtained for the quiescent fluid, which are *orthogonal* to the electric field. The orientation of the scattering lobes reflects the orientation of the chains.

The rotation angle  $\theta$  of the chains is determined by first dividing the scattering image into 360 wedges, each subtending  $1^\circ$  of arc, and then integrating to find the average intensity in each wedge [5]. The orientation of the scattering lobes is then obtained by either locating the intensity maximum,  $\theta_{\max}$ , or finding the median,  $\theta_m$ , that divides the integrated scattered intensity into equal halves, so  $\int_{\theta_m}^{90^\circ} I(\theta) d\theta = \int_{-90^\circ}^{\theta_m} I(\theta) d\theta$ . The median is useful when the dynamics is strongly nonlinear, but gives an orientation angle about 5 times smaller than  $\theta_{\max}$ , since it is greatly affected by polydispersity.

*Measurements.*—At low strain amplitudes  $\gamma_0 \ll 1$  the response of the orientation angle  $\theta_{\max}$  to the shear strain  $\gamma = \gamma_0 \sin(2\pi\nu t)$  is nearly sinusoidal. This sinusoidal response is exemplified in Fig. 1, where clockwise Lis-

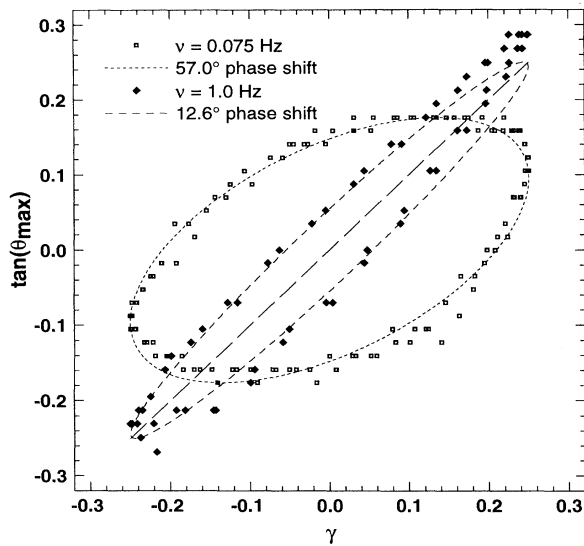


FIG. 1. Clockwise Lissajous plots of  $\tan(\theta_{\max})$  against  $\gamma$  are virtually elliptical at small strain amplitudes. At high frequency the motion is nearly in phase with the strain; at low frequency the motion is nearly in phase with the strain rate.

sajous plots of  $\tan(\theta_{\max})$  against  $\gamma$  are shown to be nearly elliptical. At high frequencies the shear rate,  $\dot{\gamma} = 2\pi\nu\gamma_0 \sin(2\pi\nu t)$ , is large, and the chain orientation is nearly in phase with the fluid shear, indicating the hydrodynamic torque on a chain dominates the electrostatic torque. Affine deformation is nearly achieved, as shown by the dashed line.

At low shear frequencies the chain orientation leads the strain by  $57^\circ$  and thus lags the strain rate by  $33^\circ$ . In

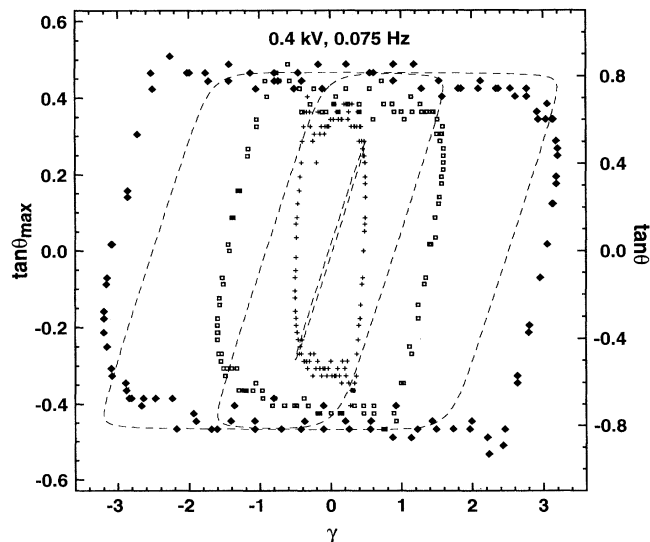


FIG. 2. Lissajous plots at strain amplitudes of  $\gamma_0 = 0.5, 1.6,$  and  $3.2$  have parallelogram shapes that indicate a “clipping” of the angular motion as chains fragment and align with the field at high strains. The theoretical curves are computed in the instantaneous “equilibrium” limit where  $k$  is large.

this regime electrostatic torque evidently dominates the hydrodynamic torque.

At higher strain amplitudes, Fig. 2, the sinusoidal motion becomes “clipped” as the chains fragment and aggregate during a cycle in order to maintain good field alignment, giving parallelogram Lissajous plots.

At lower voltages we observe the nonlinear fluid response shown in Fig. 3. Starting at maximum positive strain, the chain half cycle can be described as follows. As the strain reverses, the chains comove with the fluid, tilt to a maximum angle at half maximum strain, whereupon they fragment and undergo retrograde motion to realign with the electric field. Analysis shows that as they comove with the shearing fluid, the chains aggregate, and indeed the scattering lobes brighten considerably during this time. These observations of chain motion have led us to propose the following model of ER fluid microstructure and rheology.

*Theory.*—The salient features of the experimental results can be understood in terms of a kinetic model of the dynamics of volatile chains. In this model we assume that dipolar interactions and hydrodynamic forces dominate thermal forces, which is certainly true in our experiments. This kinetic chain model differs from the elliptical droplet model [6], which minimizes a free energy and thus is an equilibrium model.

Consider a linear chain of  $2N + 1$  spheres of radius  $a$  labeled from  $-N$  to  $N$  in a coordinate system  $(x, z)$ , the origin of which is centered on the zeroth sphere. The  $z$  axis is in the direction of the electric field, and the  $x$  axis is in the direction of fluid flow. The chain makes an angle  $\theta$  to the  $z$  axis, so the position of the  $k$ th bead is  $(2ak \sin\theta, 2ak \cos\theta)$ . The fluid velocity is given by

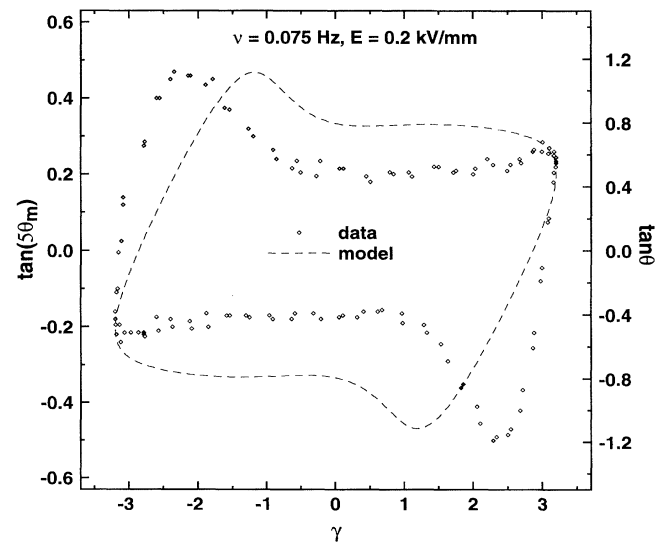


FIG. 3. At low voltages a novel retrograde motion of fragmenting chains can be observed (dashed line is theory). The amplitude of motion is sensitive to the dipolar model and the method of data reduction.

$\mathbf{v}(z) = \gamma z \dot{\hat{\mathbf{x}}}$ , where  $\hat{\mathbf{x}}$  is a unit vector, and the velocity of the  $k$ th bead is  $\mathbf{v}_k = 2ak\dot{\theta}(\cos\theta\hat{\mathbf{x}} - \sin\theta\hat{\mathbf{z}})$  for a chain rotating at angular velocity  $\dot{\theta}$ .

The shearing fluid exerts a hydrodynamic force  $\mathbf{F}_k = 6\pi\mu_0a[\mathbf{v}(z) - \mathbf{v}_k]$  on the  $k$ th bead, where  $\mu_0$  is the liquid viscosity. This force can be decomposed into a tangential component that causes chain rotation, and a radial component that causes tension or compression. The tangential component of the hydrodynamically induced force between the  $k$ th and  $(k+1)$ th spheres is  $F_{h,\theta} = \sum_{k+1}^N \mathbf{F}_k(\cos\theta, -\sin\theta) \cong 6\pi\mu_0a^2(\dot{\gamma}\cos^2\theta - \dot{\theta})(N^2 - k^2)$ . This force is a maximum at the chain center, where in low Reynolds number flow is balanced by the tangential component of the dipole-dipole interaction force,  $F_{e,\theta} = (3\pi a^2\mu_0\dot{\gamma}/8Mn)\sin 2\theta$  [9]. Here  $Mn = \mu_0\dot{\gamma}/2\varepsilon_0\varepsilon_c\beta^2E_0^2$  is the Mason number, which expresses the ratio of hydrodynamic to electrostatic forces,  $\beta$  is the dielectric contrast factor  $(\varepsilon_p - \varepsilon_c)/(\varepsilon_p + 2\varepsilon_c)$ , and  $\varepsilon_c$  and  $\varepsilon_p$  are the liquid and particle dielectric constants [9]. Balancing the tangential hydrodynamic and electrostatic forces at the chain center [10] gives the equation of motion [11]

$$\dot{\theta} + \omega_d \sin 2\theta = \dot{\gamma} \cos^2 \theta, \quad \omega_d = \dot{\gamma}/16MnN^2. \quad (1)$$

The characteristic frequency  $\omega_d$  depends strongly on chain size. Physically acceptable values of  $N$  must correspond to mechanically stable chains or fragmentation will occur. The radial component (directed along the chain axis) of the hydrodynamic force is

$$F_{h,r} = \sum_{k+1}^N \mathbf{F}_k(\sin\theta, \cos\theta) = 3\pi\mu_0a^2\dot{\gamma}\sin(2\theta)(N^2 - k^2)$$

This force, which again is a maximum at the chain center, puts the chain in tension when  $\theta\dot{\gamma} > 0$  and under compression when  $\theta\dot{\gamma} < 0$ . For the chain to be stable to fracture this hydrodynamically induced force must be smaller than the radial component of the electrostatic interaction [9]  $F_{e,r} = (3\pi a^2\mu_0\dot{\gamma}/8Mn)(3\cos^2\theta - 1)$ . The maximum stable chain number is determined by balancing these forces at the chain center:

$$N_{\max} = \begin{cases} \sqrt{\frac{2}{Mn} \frac{3\cos^2\theta - 1}{\sin 2\theta}}, & \dot{\gamma}\theta \geq 0, \\ \infty, & \dot{\gamma}\theta \leq 0. \end{cases} \quad (2)$$

$N_{\max}$  is dependent on chain orientation and strain rate, causing nonlinear response when driven by oscillatory shear  $\dot{\gamma} = 2\pi\nu\gamma_0\cos(2\pi\nu t)$ . The maximum stable chain length diverges when the chain is aligned with the field, when the instantaneous strain rate is zero, and when the chain is under compression.

If a chain finds itself far from its maximally stable size, then its size will adjust by aggregation or fragmentation. The kinetics of aggregation and fragmentation can be described by the phenomenological formula

$$\frac{dN(t)}{dt} = \frac{k}{N(t)} \left[ 1 - \frac{N(t)^2}{N_{\max}^2(t)} \right], \quad (3)$$

where because induced dipolar forces drive aggregation the rate constant  $k = k_0(8\varepsilon_0\varepsilon_c\beta^2E_0^2/\mu_0)$  where  $k_0$  is a

concentration dependent constant we treat as a free parameter. When the chain is at its maximum length no aggregation or fragmentation occurs since  $dN(t)/dt = 0$ . When the chain is much smaller than its maximum stable length, the chain will aggregate according to  $N(t) = \sqrt{N(0)^2 + 2kt}$ , in agreement with the root time prediction of See and Doi [12]. Thus aggregation is a slow power-law growth process that is independent of the often divergent size  $N_{\max}$ . If the chain is much larger than its stable length, then it will fragment exponentially quickly according to  $N(t) = N(0)e^{-kt/N_{\max}^2}$ . Note that the fragmentation rate  $k/N_{\max}^2$  is proportional to the strain rate and is independent of the electric field. Thus the phenomenological rate equation gives physically reasonable behavior, while avoiding the complexities of the Smoluchowski equation.

Equations (1)–(3) are a set of coupled equations that model the dynamics of chains in shear flow. There are four independent parameters in the system;  $Mn$ ,  $\nu$ ,  $\gamma_0$ , and  $k_0$ . A simplification occurs by noting that solutions to the kinetic equation are of the form  $N(t) = (\dot{\gamma}/16\nu Mn)^{1/2}n(\nu t)$ . Expressing all functions in terms of the dimensionless time  $s = \nu t$  this leads to the reduced equations

$$\dot{\theta} + \frac{1}{n^2} \sin 2\theta = \dot{\gamma} \cos^2 \theta, \quad \dot{n} = \frac{k_0}{n} \left[ 1 - \frac{n^2}{n_{\max}^2} \right], \quad (4)$$

$$n_{\max} = \begin{cases} 4\sqrt{\frac{2}{\dot{\gamma}} \frac{3\cos^2\theta - 1}{\sin 2\theta}}, & \dot{\gamma}\theta \geq 0, \\ \infty, & \dot{\gamma}\theta < 0. \end{cases}$$

The reduction to a two parameter  $(\gamma_0, k_0)$  model is a result of the rate equation we have chosen. Because the strain amplitude is fixed by experiment, this is really a signal free parameter model.

Before showing the behavior of these equations we would like to discuss the predicted rheology. The hydrodynamic torque  $\tau_h$  on a chain can be computed by summing the tangential component of the hydrodynamic force on each bead times its respective moment. In terms of the chain length  $L = 2a \times 2N$  the hydrodynamic torque is thus  $\tau_h = (\pi/4)\mu_0L^3(\dot{\gamma}\cos^2\theta - \dot{\theta})$ . The electrostatic torque  $\tau_e$  can be computed by recalling from the torque balance of Eq. (1) that  $\dot{\gamma}\cos^2\theta - \dot{\theta} = (\gamma a^2/MnL^2)\sin 2\theta$ ; this gives  $\tau_e = (\pi/2)a^2\varepsilon_0\varepsilon_c\beta^2E_0^2L\sin 2\theta$ . The stress  $\sigma$  in the sample is the hydrodynamic torque density, which equals the electrostatic torque density since inertia is small. In terms of the volume fraction  $\phi$  of spheres this is  $\sigma = 6\mu_0N^2\phi(\dot{\gamma}\cos^2\theta - \dot{\theta}) = \frac{3}{4}\varepsilon_0\varepsilon_c\beta^2E_0^2\phi\sin 2\theta$ . This equation demonstrates that the stress is nearly proportional to the angle  $\theta$ , so light scattering is an independent probe of stress [13]. Furthermore, it is apparent that when  $\theta = 0$ , the chain is comoving with the fluid so  $\dot{\gamma}\cos^2\theta = \dot{\theta}$ .

Because the dynamics of chain orientation  $\theta(s)$  is independent of electric field and shear frequency, we conclude that the stress scales purely as the square of the electric field. In steady shear it is readily shown that

$\sin 2\theta = 2\sqrt{6}/5$ , so the solution viscosity has the shear thinning form (after adding in the zero-field viscosity  $\mu_\phi$ )

$$\mu = \mu_\phi + \frac{3\sqrt{6}}{10} \varepsilon_0 \varepsilon_c \beta^2 E_0^2 \phi \dot{\gamma}^{-1}. \quad (5)$$

The result  $\mu \propto \dot{\gamma}^{-1}$  has been obtained in many experiments, including those conducted on our silica fluid [6]. However, for the silica fluid at low fields we find  $\mu \propto \dot{\gamma}^{-2/3}$ , a result consistent with the elliptical droplet model [6].

The nature of the nonlinear response is illustrated in Fig. 4 (small strains give a sinusoidal response) for a range of the rate constant  $k$ . For small values of  $k$  the chain reorientation rate  $\omega_d$  is essentially constant because the chains cannot restructure during a shear cycle. The remaining nonlinearities in Eq. (1) are small enough that a nearly elliptical response is observed. In contrast, for large values of  $k$  the chains fragment and aggregate rapidly to achieve mechanical stability while trying to maximize their length, and Lissajous plots approach a parallelogram, as in Fig. 2. Finally, for intermediate values of  $k$  an interesting crossover to retrograde motion is observed. This is observed in our data at low fields, as illustrated in Fig. 3. Thus the nonlinear response varies continuously with  $k$ .

The dipolar kinetic chain model gives a qualitative account of the nonlinearities observed in our data, without generating behaviors that we have not observed. However, it makes a number of quantitative predictions that are not correct, such as predicting chain angles that are too large and not accounting for residual field and fre-

quency trends in the data. It is easy to modify the theory to give much better fits to the data, for example, by rescaling  $n_{\max}$ , but only at the expense of introducing arbitrary parameters. What are the problems? Local field corrections for a system with negative contrast decrease the chain angle. The distribution of chain sizes has been ignored, yet light scattering samples all chains and thus *underestimates* the maximum chain orientation. Nonetheless, we feel that this model provides a framework that captures the essence of the observed dynamics.

We have conducted light scattering studies that show that ER fluids can have strongly nonlinear behavior in oscillatory shear. We have given a simple formulation of the nonlinearities in terms of dipolar chains that fragment and aggregate. Much of our experimental data can be described by taking the instantaneous equilibrium limit; however, at low fields strong nonlinearities suggest that the kinetics is slow. Finally, we predict the nonlinear rheology of an ER fluid.

This work was performed at Sandia National Laboratories and was supported by the U.S. Department of Energy under Contract No. DE-AC-0476DP00789. J.E.M. acknowledges helpful theory discussions with T.C. Halsey and R. Anderson, the suggestions of C.J. Martin on mechanical design of the shear cell drive, and the computer skills of C. Tigges, which resulted in a *real time* Macintosh application for the chain equations.

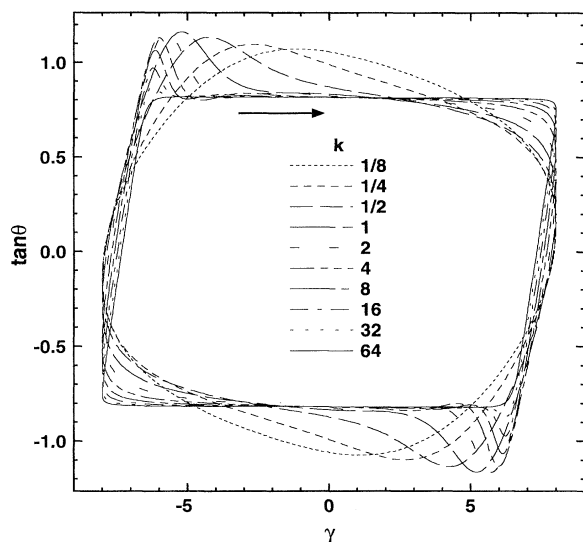


FIG. 4. Lissajous plots change unexpectedly as the rate constant  $k$  is varied. For  $k = 0$  the chain reorientation rate  $\omega_d$  is a simple constant, and the remaining nonlinearities in Eq. (1) are small enough that a nearly elliptical response is observed. For large  $k$  Lissajous plots approach a parallelogram, whereas for intermediate  $k$  values retrograde motion is observed.

- [1] H. Block and J.P. Kelly, J. Phys. D **21**, 1661 (1988).
- [2] A.P. Gast and C.F. Zukoski, Adv. Colloid Interface Sci. **30**, 153 (1988).
- [3] J.E. Martin, J. Odinek, and T.C. Halsey, Phys. Rev. Lett. **69**, 1524 (1992).
- [4] T. Chen, R.N. Zitter, and R. Tao, Phys. Rev. Lett. **68**, 2555 (1992).
- [5] J.E. Martin, J. Odinek, and T.C. Halsey, Phys. Rev. E **50**, 3263 (1994).
- [6] T.C. Halsey, J.E. Martin, and D. Adolf, Phys. Rev. Lett. **68**, 1519 (1992).
- [7] J.E. Martin, D. Adolf, and T.C. Halsey, J. Colloid Interface Sci. **167**, 437 (1994).
- [8] T.C.B. McLeish, T. Jordan, and M.T. Shaw, J. Rheol. **35**, 427 (1991); T. Jordan, M.T. Shaw, and T.C.B. McLeish, J. Rheol. **36**, 441 (1992).
- [9] D.J. Klingenberg and C.F. Zukoski, Langmuir **6**, 15–24 (1990).
- [10] Balancing the force along the chain gives a chain shape that resembles an arcsine; linearity avoids a dynamical system of  $2N + 1$  coupled nonlinear equations.
- [11] A similar result is obtained from the droplet model in Ref. [6].
- [12] H. See and M. Doi, J. Phys. Soc. Jpn. **60**, 2778 (1991).
- [13] This is analogous to the stress-optical theorem, which relates birefringence to stress.